SurfPower parametric design study: part I

Ryan Nicoll
November 6, 2009

www.dsa-ltd.ca

Ryan Nicoll, Director
PO Box 3075, STN CSC
Victoria, BC V8W 3W2
p.250.472.4323
f.250.721.6497
ryan@dsa-ltd.ca

Seawood Designs Inc.
Charles Wood, Director
p.250.743.7107
seawood@shaw.ca

Table of Contents

List of Figures

List of Tables

1 Introduction

Seawood Designs, Inc. (SDI) is developing an ocean wave energy capture device called SurfPower. The device consists of a large pontoon which is actuated by passing ocean waves. The device pumps seawater into a high pressure hydraulic system that drives a turbine to generate electricity. Conceptual diagrams of the SurfPower pontoon and system layout can be seen in Figure 1 and Figure 2 respectively (courtesy of SDI).

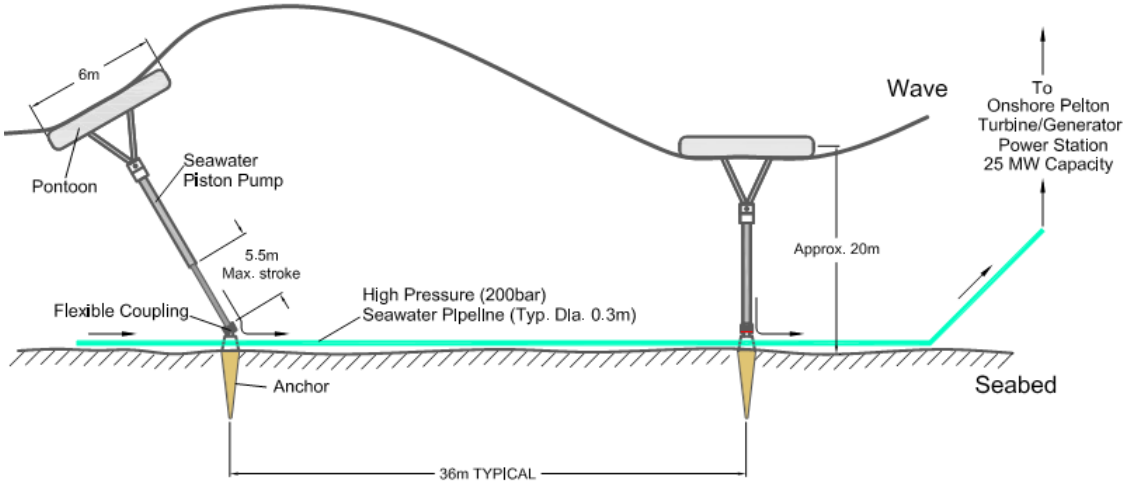

Figure 1: Pontoon operation

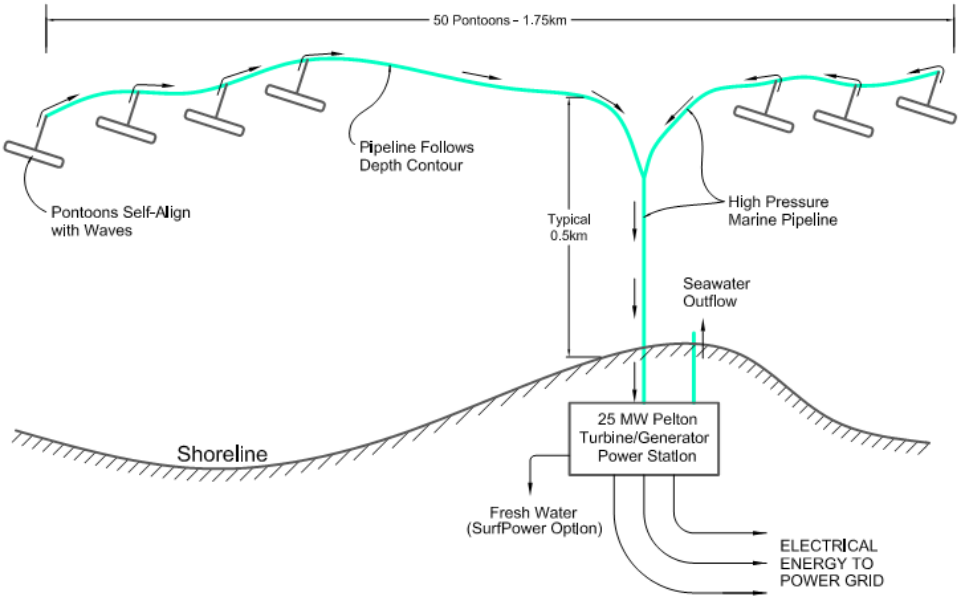

Figure 2: System layout

Dynamic Systems Analysis, Ltd. (DSA) has extensive experience with high-fidelity time domain simulation of mechanical systems in marine environments. Seawood Designs retained the services of DSA to undertake dynamic simulation studies for a SurfPower system that was specifically configured to yield optimum energy recovery in moderate sea states (1-4 meters). This design would be most suitable at lower latitudes where energy flux levels tend to be lower and the systems could be deployed to deliver electrical energy and in some cases drive reverse osmosis desalination plants. This SurfPower configuration has the advantage of maximizing energy availability.

This report summarizes the work completed by DSA through an accurate simulation-based parametric design methodology on the SurfPower technology. An extensive list of combinations including different pontoon shapes, materials, equivalent hydraulic system operating pressures, and environment conditions have been tested to define the system performance.

Seawood Designs Inc. has requested the final report be issued in two parts. The first part SDI will make available to any party interested in wave energy; the second part has to remain confidential for now as this material may be the subject of future patents and ongoing studies.

2 Definitions

The following terms are used throughout the proposal to describe the device design:

1. **hydraulic freeboard:** the freeboard required to provided sufficient buoyancy to statically oppose the nominal hydraulic system pressure
2. **dynamic freeboard:** the additional freeboard in excess of the hydraulic freeboard that is required to accelerate the system in response to oncoming waves
3. **total freeboard:** the sum of hydraulic and dynamic freeboards
4. **reserve buoyancy:** the portion of the pontoon that remains out of the water in a particular sea state condition
5. **end stop condition:** when the pontoon is near or impacts with system end stops
6. **offset:** the distance between the center of buoyancy and the cylinder connection point on the pontoon assembly
7. **run:** simulation of the passage of a minimum number of waves required to establish consistent steady-state dynamic behavior of the system

3 Design strategy outline

This section presents the numerical tools and the methodology that were used to study the system.

3.1 Methodology review

The primary design tool DSA used to evaluate the SurfPower system is a numerical simulation testbed called ProteusDS that incorporates articulated rigid body models and non-linear elastic cable / beam dynamics models. All models used in ProteusDS are based on techniques presented in peer-reviewed scientific journals. Once a particular system is set up for simulation, many different sets of environment conditions, including different ocean waves and currents, can be applied and the resulting

dynamic response of the system can be observed. The dynamic response incorporates information on forces present in the system, the motion of the pontoons, and the energy captured. This process gives significant insight on the behavior of the pontoon during normal operational and extreme sea states.

For the work presented here, the simple pontoon shape seen in Figure 1 was studied. The unmodified simple pontoon shape will be analyzed to serve as a benchmark design to compare modified pontoon designs against.

3.2 System model

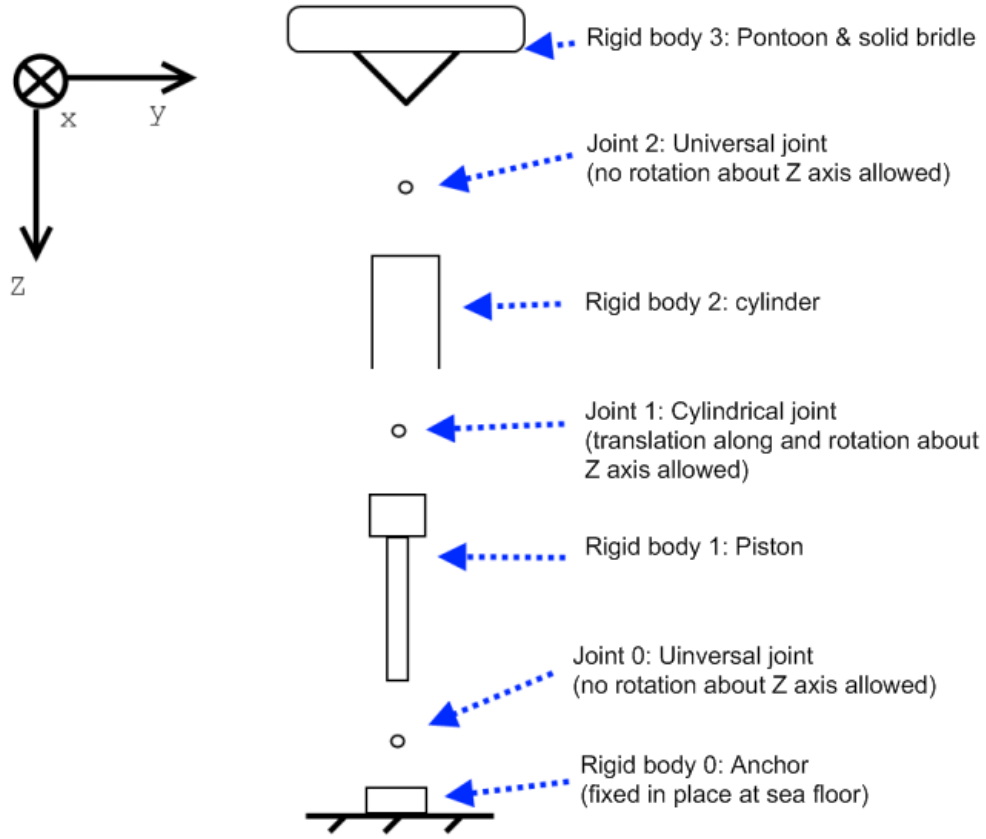

Figure 3: Articulated SurfPower model

The system was modeled as an articulated rigid body system. Each body and sequential joint used in the system is mapped in Figure 3.

Several pontoon designs were tested, which include variations in geometry and materials. The two pontoon shapes tested can be seen in Figure 4 and Figure 5. The intent of the tapered pontoon shape is to maintain its orientation to the waves due to the angled end faces. In Figure 6, the key body directions are illustrated along with the typical alignment relative to propagating waves.

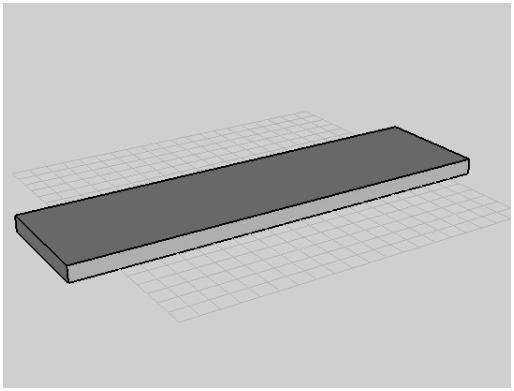

Figure 4: Simple rectangular pontoon

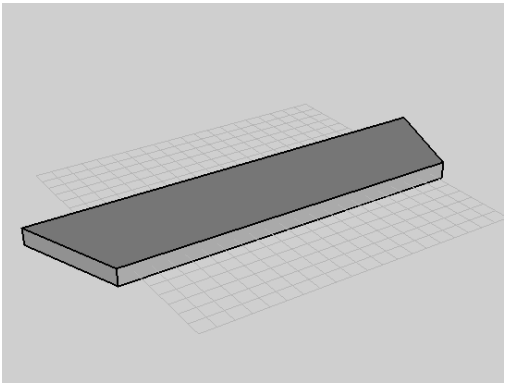

Figure 5: Tapered pontoon

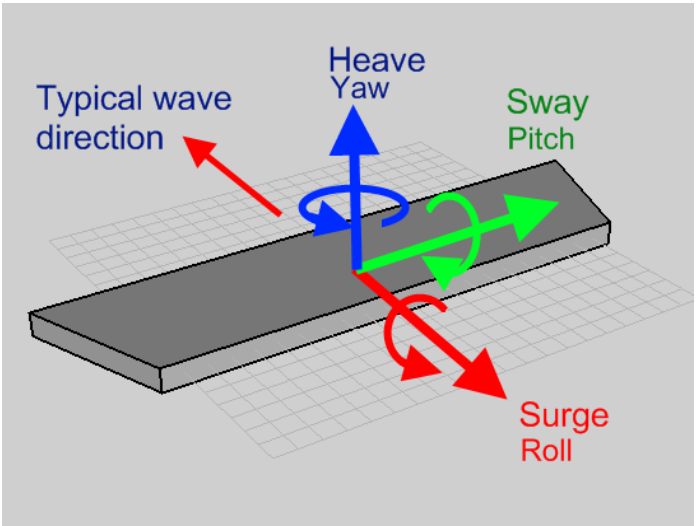

Figure 6: Pontoon movement directions

Both pontoons were tested in steel and aluminum versions: the aluminum version has roughly half the mass and inertia values of the steel pontoon as well as a slightly smaller total freeboard to account for the smaller weight of the system. Mass values were estimated by SDI. Inertia values were estimated

using the simple pontoon dimensions and assuming a homogenous density. This will underestimate the actual inertia values as in reality the mass was concentrated around the skin of the device, but the rotational motions are not as important to system performance as heave and surge. The mass properties of the pontoons are summarized in Table 1. Pontoon dimensions for the simple and tapered designs are summarized in Table 2.

Table 1: Pontoon mass properties

	Mass (kg)	Roll Inertia (kg m^2)	Pitch Inertia (kg m^2)	Yaw Inertia (kg m^2)
Steel	3.18E+004	1.60E+006	1.20E+005	1.70E+006
Aluminum	1.77E+004	8.80E+005	6.70E+004	9.40E+005

Table 2: Pontoon dimensions

	Max Length (m)	Max Width (m)	Height (m)	Taper angle
Steel	24.400	6.700	1.067	0.000
Steel tapered	26.800	6.700	1.067	20.000
Aluminum	24.400	6.700	0.889	0.000
Aluminum tapered	26.800	6.700	0.889	20.000

To model the reaction load from the hydraulic system, a constant joint force (a force that is applied along the line of action of the joint) was applied to the cylinder body only when the joint had a positive (extension) velocity. The magnitude of the force was the product of the current hydraulic system pressure and the piston area, which for each run was constant. In addition to these joint forces, a constant friction force was applied to the cylinder joint of 9 kN.

Hydrodynamic drag loading was modeled on the piston rod and cylinder by applying the Morison equation on discrete strips along the cylinders. This produces the appropriate drag and added mass effect of these components. Hydrodynamic and buoyancy modeling is more difficult for the pontoon shape due to the dynamic submergence of the body and complex relative velocity between the pontoon surface and the water particles. However, a relatively simple method for accurately quantifying buoyancy and Morison-type loading on the pontoons in a discretized manner is used regularly by DSA. The pontoon surface is broken up in to many discrete panels, such as the tapered pontoon seen in Figure 7. The unit normal, area, and location with respect to the center of mass of each panel is known. To quantify buoyancy, the subsurface ocean pressure, which is a function of the hydrostatic pressure and the pressure disturbance from the presence of ocean waves, is found and applied at the centroid of each panel. The resulting process is effectively a discrete approximation to a surface integral and provides a very accurate buoyancy force and moment. To quantify Morison-type loading, the relative velocity between the body and fluid at each panel centroid is found and a hydrodynamic force and moment (included added mass effects) are quantified and applied on the body. This is a robust,

scalable, and accurate method for evaluating these complex forces as the body experience variable submergence throughout the simulation. Due to the shape of the pontoon, a sensitivity study on the added mass and drag coefficients to be used was completed to observe the effect on power capture. The resulting coefficients used for all surface panels was a drag coefficient of 1.0 and added mass coefficient of 1.0.

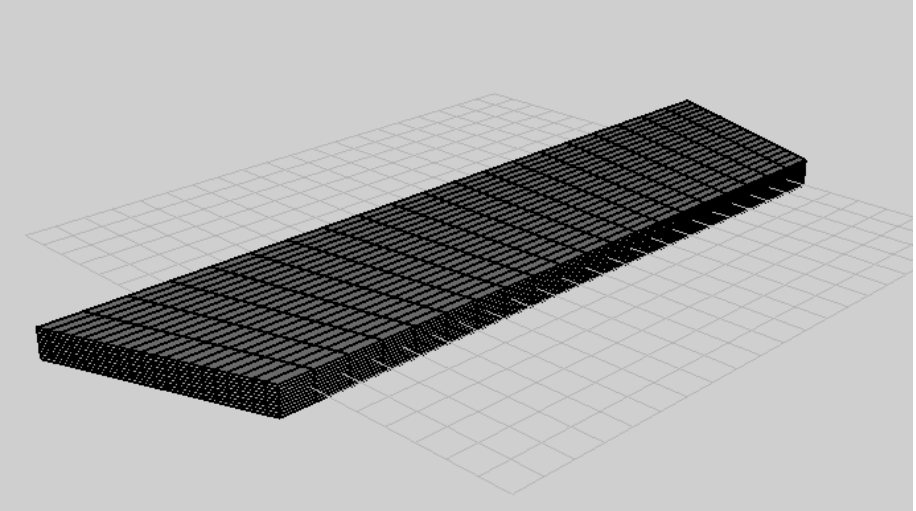

Figure 7: Tapered pontoon hydrodynamic and buoyancy mesh

3.3 Environment conditions

Several key environment conditions were used that had been specified by SDI. The nominal operating design sea state is characterized by a wave height (trough to crest) of 3.7 m and period of 6 and 11 s. The extreme design sea state is characterized by a wave height of 8 m and period of 15 s. In all runs, Airy (sinusoidal) waves will be used to simplify the design process and produce well-defined performance metric values. However, several runs of device operation in more realistic spectral sea states were executed to establish more reliable energy capture numbers after optimal parameters had been determined.

In 18 m of water, the wavelengths of 6 s and 11 s period wave are 54 m and 131 m, respectively. With a pontoon width fixed at 25 m, diffraction loads can be safely neglected in 11 s waves but not in 6 s waves (i.e. $\lambda/D > 5$, where D is the characteristic dimension, and λ is the wavelength of a 10 seconds wave in 18 m water) [Faltinsen, 1990]. The dominant loads for this structure in a 11 s period will be due to added mass, buoyancy, and drag. The dominant loads for this structure in a 6 s period wave will include diffraction and reflection effects, which are not modeled in ProteusDS. Because of this, it should be noted that the results from 6 s wave period will be less accurate than 11s wave period simulations.

- wave period: 6 and 11 s
- wave height: 3.7 m (12 ft) and 8 m (26 ft)
- mean operating depth: 18 m (60 ft), 26 m (85 ft), and 34 m (110 ft)
- spectral sea state: JONSWAP with significant wave height 3.7 m and 8 m and 11 s dominant

period

3.4 Variable and fixed design values

There are several design values that must be established in simulation before any additional performance criteria can be measured:

1. optimal hydraulic system pressure resistance in increments of 25 psi
2. minimum offset: 1.22 m (4 ft), 1.98 m (6.5 ft), 2.74 m (9 ft)

Rather than adjust the pontoon geometry and hold constant the system pressure to establish the appropriate freeboard values, the hydraulic system pressure was varied with a constant pontoon geometry. The resulting freeboard values at the respective optimal hydraulic system pressures (discussed in §4.2) are compiled in Table 3.

Table 3: Pontoon freeboard

	Hydraulic freeboard (m)	Dynamic freeboard (m)	Total freeboard (m)	Total pontoon height (m)
Steel	0.744	0.080	0.824	1.067
Aluminum	0.677	0.053	0.730	0.889

The optimal system pressure was required to establish maximum power capture for each pontoon. Maximum joint travel was a key design variable and the throw range of the main cylinder was recorded for each case. Sensitivity of the system performance to the offset value was tested to establish the stability response of the system during extreme waves.

Fixed system parameters include:

- maximum cylinder stroke: 5.5 m (18 feet)
- pontoon weight: provided by SDI
- pontoon dimensions: provided by SDI
- pump, cylinder and piston rod dimensions and mass: provided SDI

3.5 Performance metrics

Once the critical design values were established, the key performance metrics of different pontoon designs were measured. The key performance metrics that were measured in all runs were:

- Energy recovery
- Maximum pump cylinder velocity
- Maximum angular deflection of the pump cylinder

4 Results and discussion

Analysis of the system in varying sea states and operating depths produced many interesting insights into the device operation. The following presents and explains some of the dynamic behavior characteristics of the system.

4.1 Pontoon sway instability

An important and unanticipated effect was observed. Even when the system is perfectly aligned to propagating waves, the system may by susceptible to sway resonance. The cause of this behavior is due to the surge/sway natural frequency of any moored system, which is a function of the stiffness provided by the mooring reaction load and the mass – both physical mass of the pontoon and virtual masses supplied by surrounding water. This effect is caused by parametric excitation, or disturbances in the inertial and damping characteristics of the system in the sway direction that cause this motion in the absence of direct explicit forcing. It is a well-known phenomenon and experimental studies can be found in the literature [Radhakrishnan, 2007].

Sway oscillations were observed in both the steel and aluminum pontoon systems. The sway oscillations that built up reduced the power capture of the device. Fortunately, the sway instabilities can be anticipated as they are a function of the mooring depth, mooring reaction force, and mass properties of the system. With proper design, sway oscillations may be avoided. The surge/sway natural frequency of a completely submerged undamped buoy is given by [Radhakrishnan, 2007]:

$$\omega_n = \sqrt{\left(\frac{(B-mg)}{(mg+aB)}\frac{g}{l}\right)} \tag{1}$$

where B is buoyancy, m is the buoy mass, l is the mooring line length, g is acceleration due to gravity, and a is the added mass coefficient. Note that this equation does not consider the influence of ocean waves. An equivalent form of this equation is:

$$\omega_n = \sqrt{\left(\frac{T}{(m+a\,p_w V)\,l}\right)} \tag{2}$$

where T is mooring line tension, p_w is seawater density, and V is submerged float volume: the tension in the mooring line provides the restoring force and the mass and added mass of the buoy provide the total inertial resistance. Estimates for the natural frequency can be made if the mooring reaction load is approximated by the resistance load from the hydraulic system pressure. For simplicity, added mass is neglected. The natural frequencies of the system in various depths from 20 m to 75 m water depth as given by equation 2 are compiled in Table 4.

Table 4: Calculated steel pontoon surge/sway natural frequencies at 1000 psi

Depth (m)	ω_n (rad/s)	T_n (s)
20	1.18	5.31
25	1.06	5.94
35	0.89	7.03
50	0.75	8.4
75	0.61	10.3

A depth sensitivity of system performance at 1000 psi was completed for the steel pontoon. Average captured powers and pontoon surge values in different operating depths are summarized in Table 5.

Table 5: Average captured power at 1000 psi in 3.7m, 11s Airy waves

Depth (m)	Average captured power (kW)	Pontoon sway amplitude (m)	Pontoon surge amplitude (m)	Pontoon mean surge (m)
20	313	7.5	11	1.5
25	324	1.9	11	1.9
35	313	0.02	9.6	2.5
50	290	0.14	8	3.2
75	272	10.8	6.8	4.2

The time history of sway motions of the steel pontoon in various water depths with 3.7 m, 11 s Airy wave forcing only in the surge direction can be seen in Figure 8. The time-dependent sway oscillation magnitudes showcase this particularly strongly nonlinear behavior. The pontoon shows a strong response as the system approaches 20 m and 75 m, but not in between these depths. This emphasizes the harmonic nature of the problem: at 75 m the ocean wave stimulates the first mode (10.3 seconds) while at 20 m the first mode is again stimulated at close to half the natural frequency value. Since the aluminum pontoon is lighter, the natural frequencies tend to be stimulated in smaller wave periods, which was observed during tests with 6 second waves.

Almost no sway oscillations are present in depths of 35 to 50 m as indicated in Figure 8 and Table 5. However, the energy capture decreases by 7% as the depth increases. The energy losses are due to a decrease in surge amplitude. The pontoon surge behavior is plotted in Figure 9 and Table 5, which shows the surge amplitude decrease while mean surge position is increasing. In deeper waters with constant wave height and period, the wavelength of the ocean waves increases. The lower wave steepness in larger depths results in reduced forcing from the weight of the pontoon during the return stroke and explains the reduction in surge and power capture. Since skin friction and wind loading was not modeled, the surge amplitude could be decreased even further in reality. In addition, the large sway oscillations present in 20 m but significantly decreased in 25 m depth show an impact on power capture.

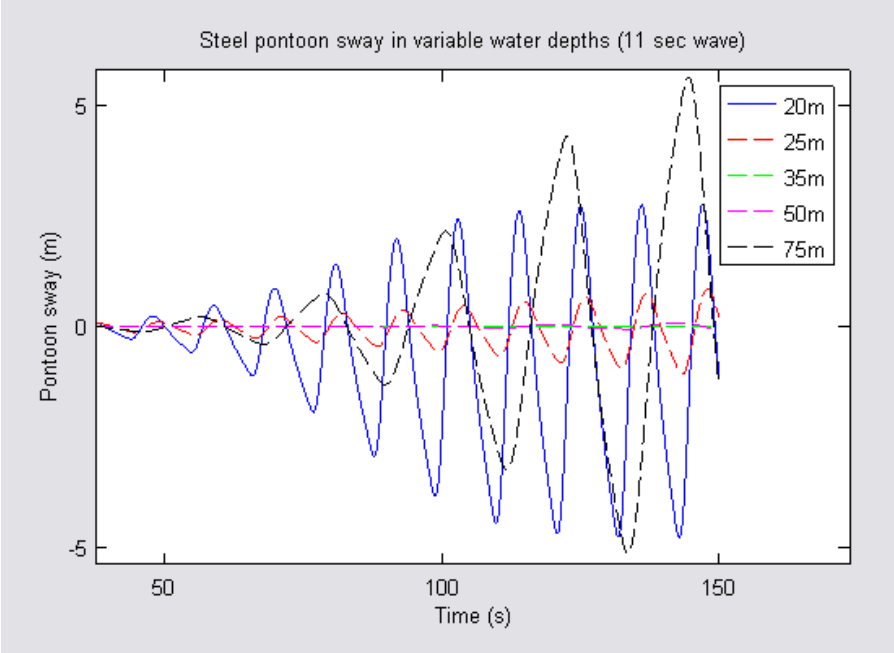

Figure 8: Steel pontoon sway in various operating depths

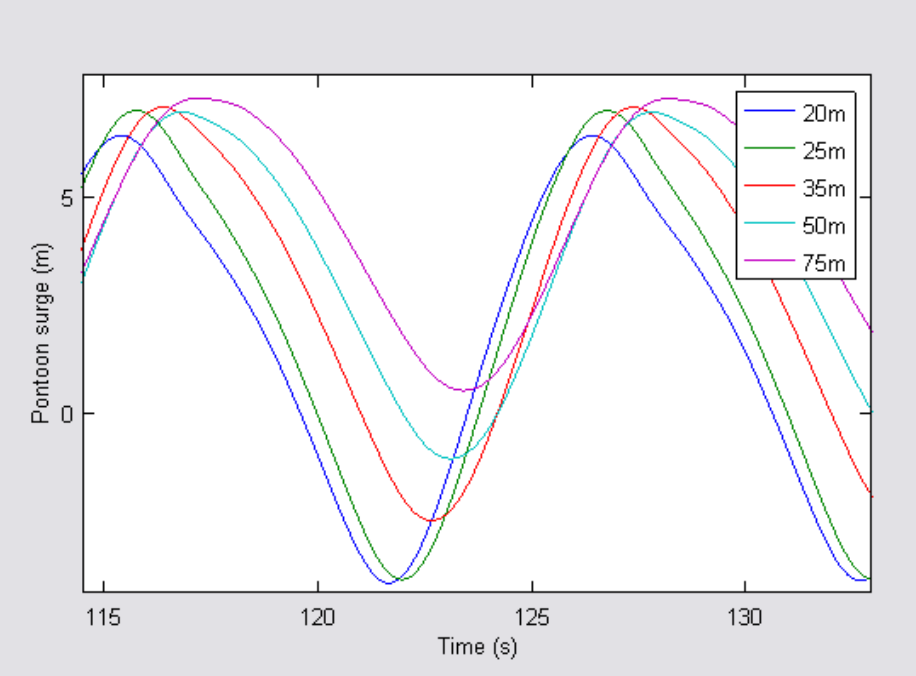

Figure 9: Pontoon surge changes with operating depth: amplitude decrease with mean value increase

As hydraulic system pressure increases, the equivalent mooring stiffness increases as well, which increases the natural frequency (or lowers the natural period). This resulted in smaller sway oscillation magnitudes. This in turn makes it much less likely to encounter resonance at full or half the natural frequency of the system. In general, large sway oscillations inhibit the device's ability to capture energy and should be avoided if possible.

4.2 Optimal hydraulic system pressure

The optimal hydraulic system pressure was obtained by executing several runs each with different constant pressure values. With a single Airy wave stimulating the system, a periodic motion of joint extension was observed. This in combination with the constant hydraulic system resistance force made calculating the captured power averaged over a single wave period very simple. The steady-state average captured power was established and sensitivity studies on hydrodynamic forcing coefficients was tested to establish appropriate values to use for the remaining simulation runs. The optimal hydraulic system pressure obtained for the steel and aluminum pontoons was 1375 psi and 1250 psi, respectively. Since in reality the final SurfPower system will not be able to adjust the global operating pressure very easily, these optimal pressure values are used for the remainder of the simulations studying the system performance in a variety of environmental conditions.

In general the heave response of the pontoon was not heavily influenced by the change in hydrodynamic drag and added mass coefficients. However, surge amplitude and mean surge position were. Usually a larger surge amplitude increases the power capture as longer joint extensions are achieved. However, the mean surge position also plays an important role. This is clarified with the use of Figure 10: the dotted lines show the approximate pontoon path traced out during the power stroke as a wave passes by. If both pontoons surge to the same downstream point, indicated by the “finish” label, a slightly longer power stroke is realized if the pontoon begins the cycle directly above the anchor point. This is because the joint is at minimum extension at this position, and as the pontoon surges towards the finish point it also moves upward in heave, further extending the joint. In Figure 10, the green path has a mean surge position that is farther downstream than the blue path. Note that wind loading and skin friction drag are not incorporated in the model to reduce the complexity of the analysis process. In long crested seas, wind loading will likely be aligned to the wave propagation direction, which would work against the return stroke of the pontoon proportional to the amount of freeboard available.

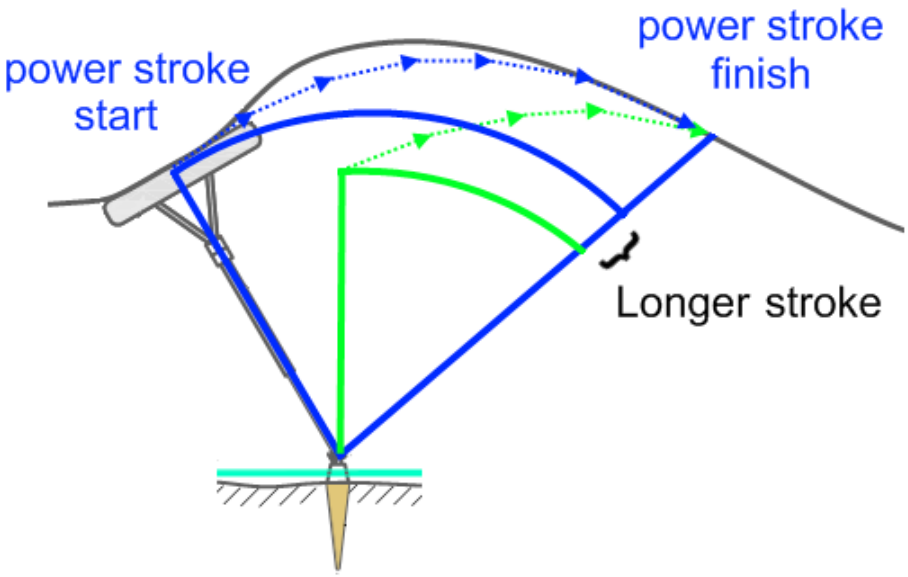

Figure 10: Longer power stroke distance realized by starting directly above anchor. Fluid skin friction and wind loading are not accounted for and may reduce the overshoot the model predicts.

4.2.1 Power capture sensitivity to added mass coefficient

A sensitivity analysis with a 3.7 m, 11 s Airy waves was completed on the added mass coefficient of the pontoon and the results are compiled in Table 6. The hydraulic pressure was held constant at 1000 psi and the drag coefficient at 1. Inspection of the pontoon surge shows that heave and surge amplitude do not significantly change, but downstream surge position moves to a more ideal configuration such as that seen in Figure 10. Surge plots for the different pontoons can be seen in Figure 11 and joint extension plots can be seen in Figure 12. The anchor is directly below the pontoon when the surge is 0. In Figure 12, the joint extension peaks are "clipped" due to the friction value set in the cylinder joint.

The physical mechanism for increase in mean surge position is due to fluid acceleration forcing (Froude Krylov forcing) on the pontoon. This forcing is proportional to the absolute acceleration of the adjacent fluid particles. During the power cycle, as the pontoon rides up the oncoming wave, there is a component of fluid particle acceleration that points in the downstream surge direction and helps increase the downstream surge value. However, once the pontoon is done the power cycle at the crest of the wave, the hydraulic system reaction load is removed and the pontoon rises up out of the water. As the pontoon moves down the back of the wave, it is less susceptible to the reversed fluid inertial forces that would push it back upstream since there is less wetted area exposed. A diagram of the water particle velocity and acceleration directions relative to the wave surface can be seen in Figure 13: note that downstream pontoon surge direction is toward the right on this diagram.

Table 6: Aluminum pontoon captured power variation with added mass coefficient (CAc)

CAc	0	1	2
Average captured power (kW)	218	271	345

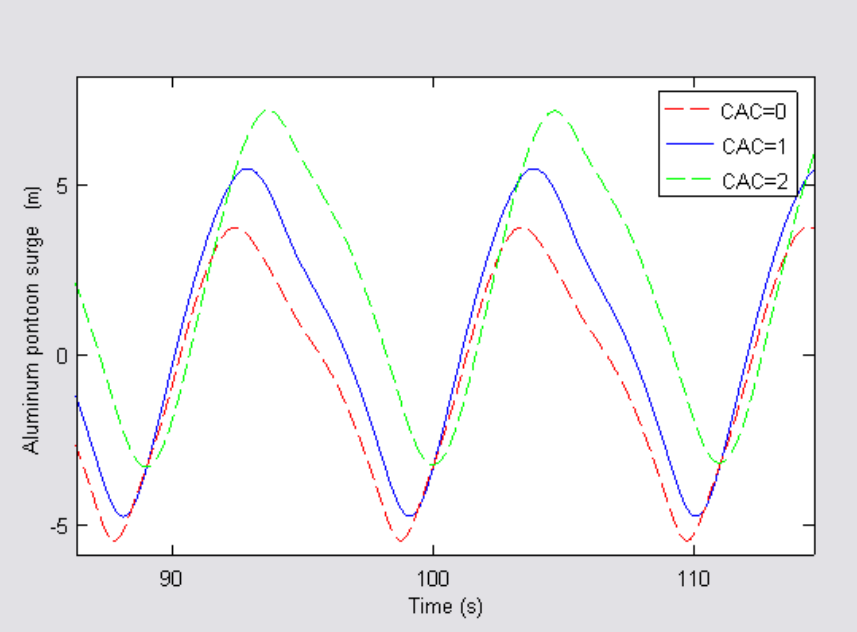

Figure 11: Pontoon mean downstream surge increase with added mass coefficient in 3.7m 11s Airy waves

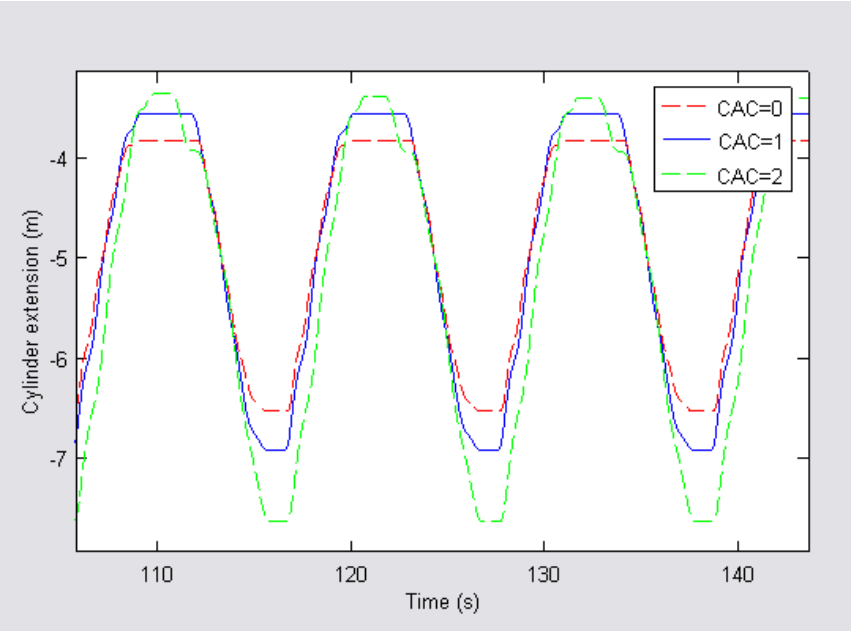

Figure 12: Aluminum pontoon joint extension increase with added mass coefficient

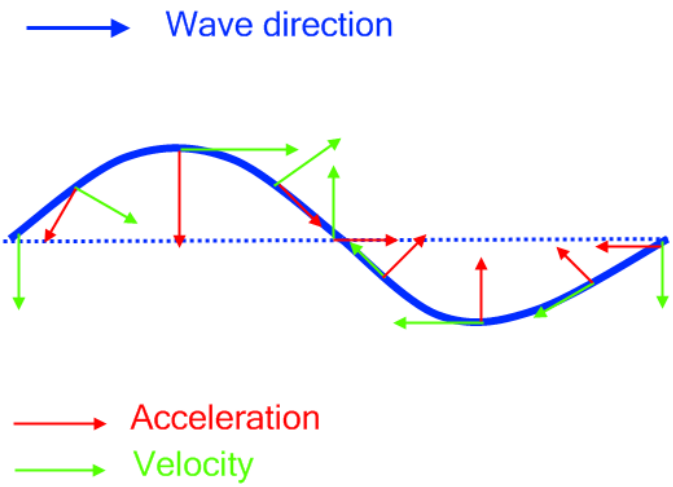

Figure 13: Water particle velocity and acceleration in a wave

An added mass coefficient of 1.0 was selected to ensure this important hydrodynamic effect was included without unrealistically increasing the expected power capture. It should be noted that typical added mass coefficients for large ocean vessels can range between 1.0 to 2.0 [Hem Lata, 2007]. The added mass coefficient will be a function of the Keulegan-Carpenter number, a dimensionless constant that indicates the importance of inertial forces to viscous forces for a body in an oscillatory flow (such as in ocean waves). Accurately establishing the added mass coefficient over a wide range of

environmental conditions will require experimental validation and is beyond the scope of this project.

4.2.2 Power capture sensitivity to drag coefficient and operating pressure

In order to establish optimum hydraulic operating pressure, the system was tested in Airy waves with 3.7 m (crest-to-trough) height and 11 s period. An image of the system from high quality rendering in these conditions can be seen in Figure 14. The average captured power of the steel and aluminum pontoons as a function of hydraulic system pressure and pontoon drag coefficient can be seen in Figure 15 and Figure 16. Note that the power stroke falls off precipitously, especially with the aluminum pontoon, after the optimal power is reached. This attribute is utilized by SurfPower to limit power capture and stroke length in higher sea states.

Figure 14: SurfPower device in 3.7 m, 11 s Airy waves

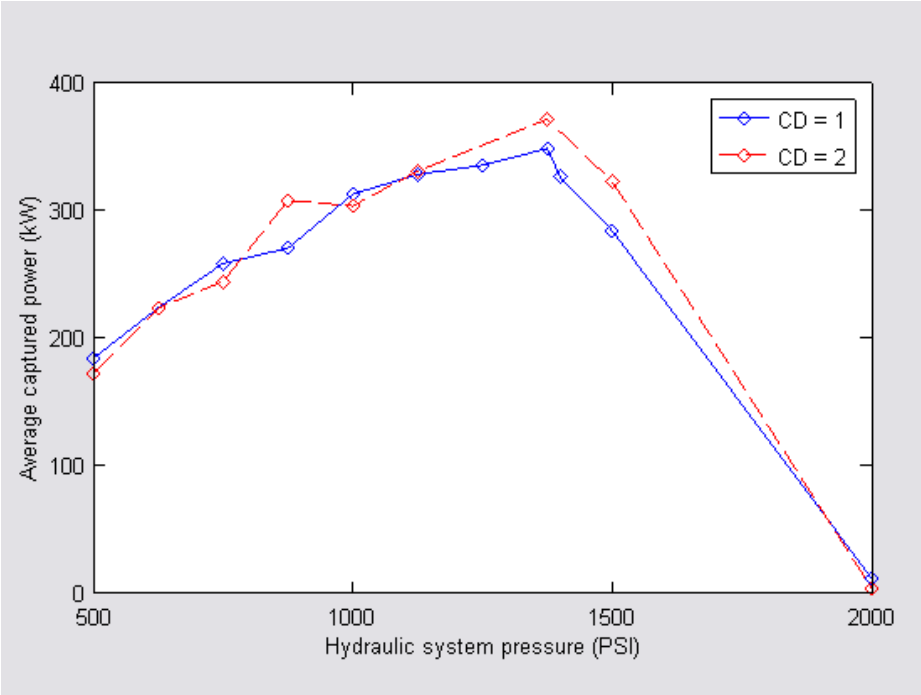

Figure 15: Steel pontoon power capture sensitivity to drag coefficient and hydraulic system pressure in 3.7m, 11s Airy waves

Optimal power capture appears to be at 1250 psi for the aluminum pontoon and 1375 psi for the steel pontoon. At lower hydraulic pressures, the power capture is similar which can partially be attributed to the presence of sway oscillations. However, at higher hydraulic pressures where sway oscillations are stifled, the power capture is greater with a larger drag coefficient. This is due to greater surge amplitudes as well as in some cases larger downstream mean surge position: both of these effects usually result in increases in joint extension amplitude and greater energy capture. Overall, the lower operating pressure requirement of the aluminum pontoon means lower component internal forces and reduced anchoring requirements as a result, which is a significant advantage over the steel pontoon.

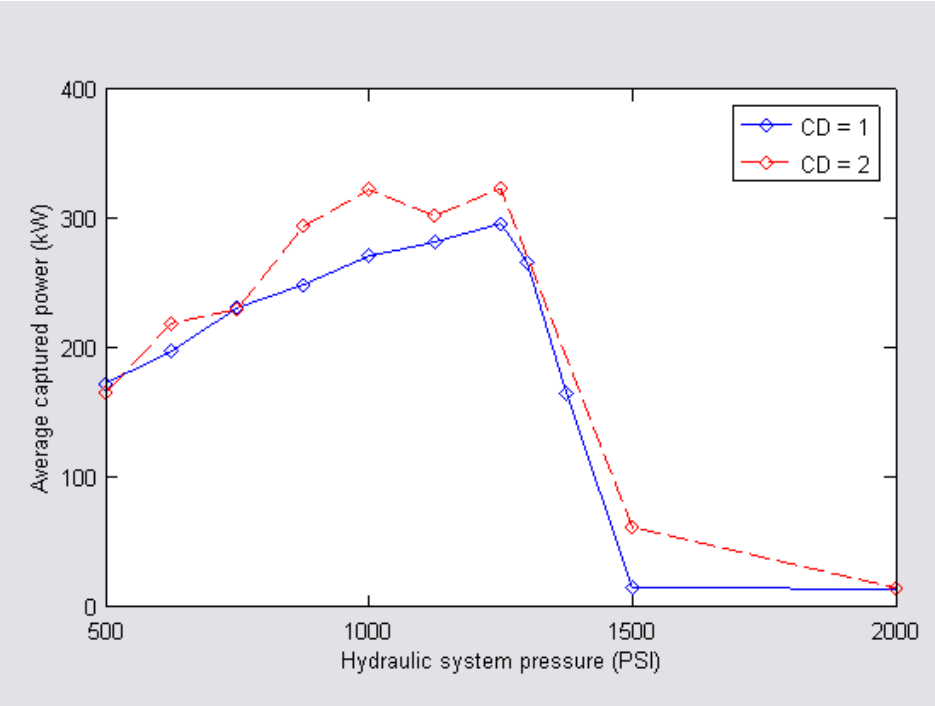

Figure 16: Aluminum pontoon power capture sensitivity to drag coefficient and hydraulic system pressure in 3.7m, 11s Airy waves

Drag coefficients will be a function of Reynolds number, a dimensionless parameter indicating the ratio of viscous forces to inertial forces in a non-oscillatory flow, and surface roughness of the pontoon system and components. However, for bluff bodies, typical drag coefficient ranges from 1.0 to 2.0. For this study, a value of 1.0 was used to ensure conservative power capture results.

Minimal differences were observed between power capture of the simple and tapered pontoon shape. The remainder of simulations used the tapered pontoon shape unless specified otherwise.

A run was completed at 1000 psi with an Airy wave with 2m, 5s propagating perpendicular to the 3.7 m, 6 s wave. The power capture in the system with the orthogonal wave was approximately 25% higher, which is due to energy captured by the extra orthogonal waves. This shows the system appears to be robust enough to capture energy in spite of disturbances from orthogonal directions.

4.3 Nominal system response and energy capture

In this section, power capture measurements with the constant hydraulic system pressure are made with variations in Airy wave height and sea state.

4.3.1 Power capture in monofrequency sea state

Power capture of the steel and aluminum pontoons in airy waves of various heights and periods can be seen in Figure 17. It should be noted that the general shape and range of values of the plots are similar to that anticipated by SDI. The power capture of the device per cubic meter of volume, or power capture density, of the device can be seen in Figure 18. The power capture density is a helpful

metric to compare different pontoons and other point absorber technologies: larger displacements incur larger mooring costs, system component costs, require heavier equipment to handle the devices, and have greater surface area to protect against corrosion and manage biofouling. The average energy capture per Airy wave can be seen in Figure 19. In general, the steel pontoon is able to capture more power and energy than the aluminum pontoon. However, the smaller total volume of the aluminum pontoon showcases a larger power density over the steel pontoon.

Another method of comparing power capture is by measuring it against the available power in the incoming waves. The power available in Airy waves is given by:

$$P_w = H^2 T \tag{3}$$

where P_w is wave power flux in kW/m (per meter crest length), H is Airy wave height (m), and T is Airy wave period (s). There are several methods to establish the equivalent 'capture width' of the SurfPower device. In light of the benefits of comparing captured power / device volume, the capture width is selected as the cube root of the pontoon and cylinder volumes. The normalized (dimensionless) power capture is therefore:

$$C_p = \frac{P_d}{P_w V} \tag{4}$$

where C_p is the normalized dimensionless volumetric device power capture coefficient, P_d is the device power captured, and V is the pontoon and cylinder volume. The resulting normalized power capture for the SurfPower devices in different Airy wave conditions is illustrated in Figure 20. Capture coefficients of greater than 1 indicate that the device is extracting a substantial portion of the incoming wave energy and will in fact be affecting waves that pass in a region adjacent to the device. Recall that wave diffraction and radiation effects are not considered in the simulation model and that these effects are expected to be important at Airy wave periods of 6 seconds. These forces will likely act to inhibit the device power stroke and thereby reduce the power capture coefficient in 6 second wave periods. In addition, Airy waves are less accurate for modeling steep ocean waves, and the smaller period and shorter wavelength waves at 6 seconds have a substantial wave steepness increase compared to the 11 second period waves. More complex wave models can be used in ProteusDS to better establish the ocean wave shape and the impact on power capture in steep waves in future studies.

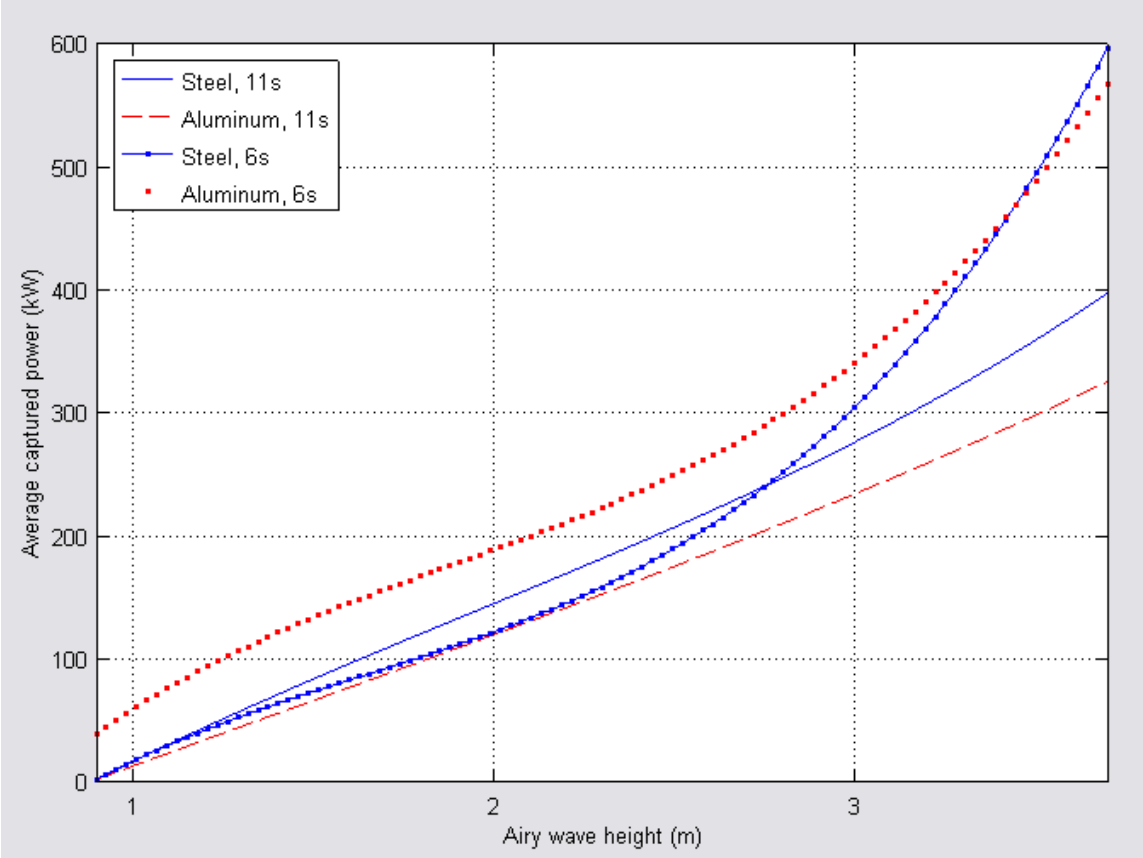

Figure 17: Pontoon power capture in Airy waves

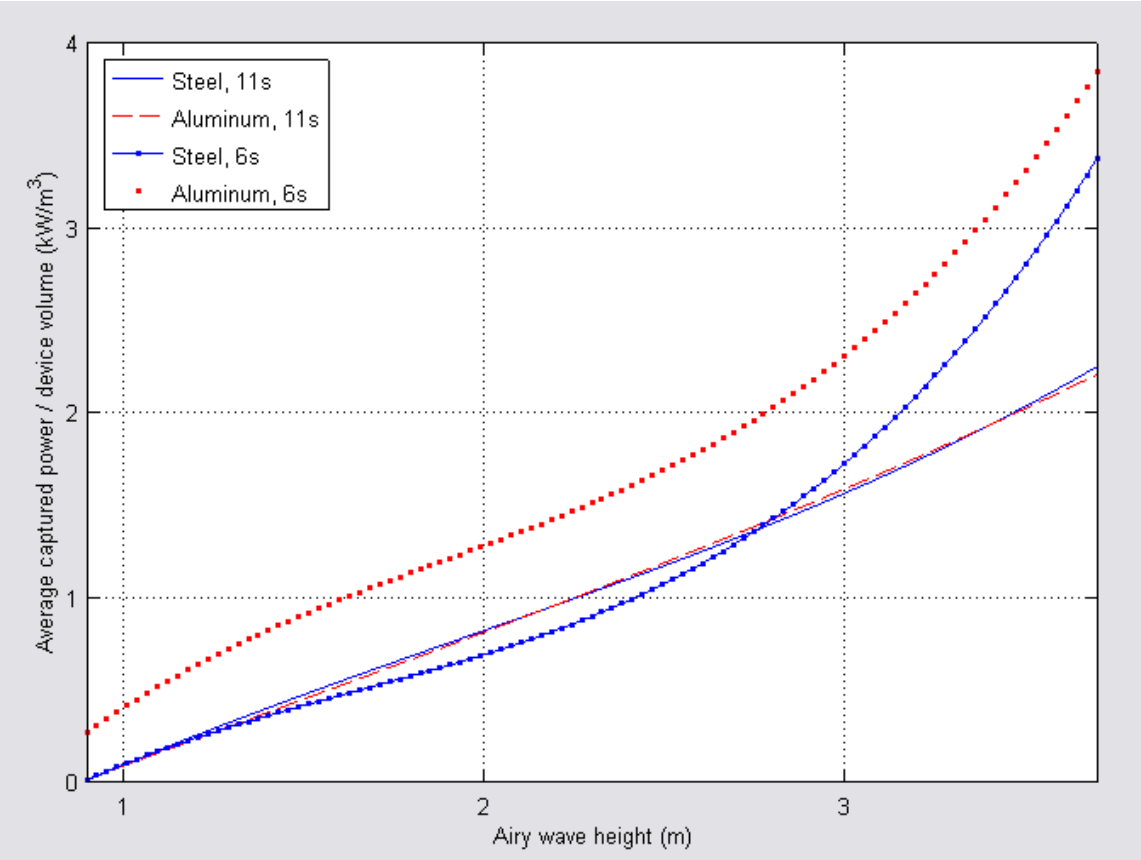

Figure 18: Pontoon power capture per device volume in Airy waves

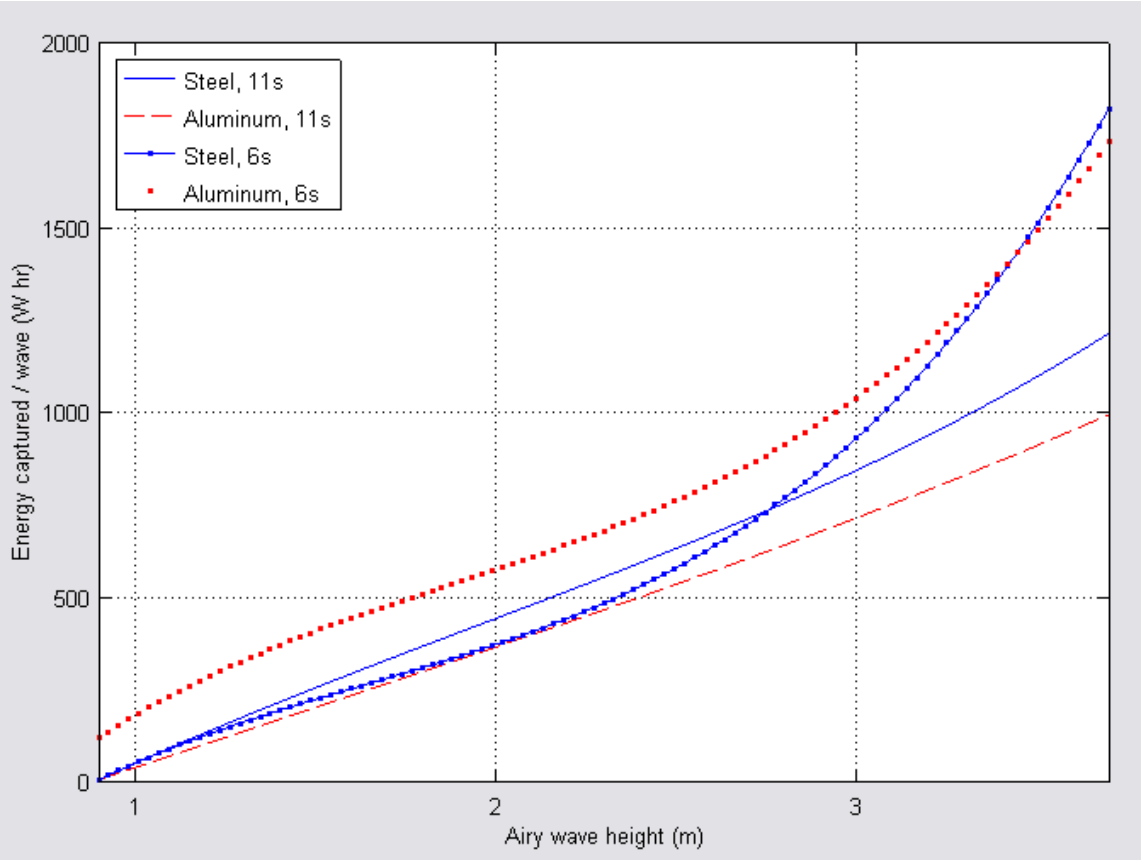

Figure 19: Pontoon energy capture per Airy wave

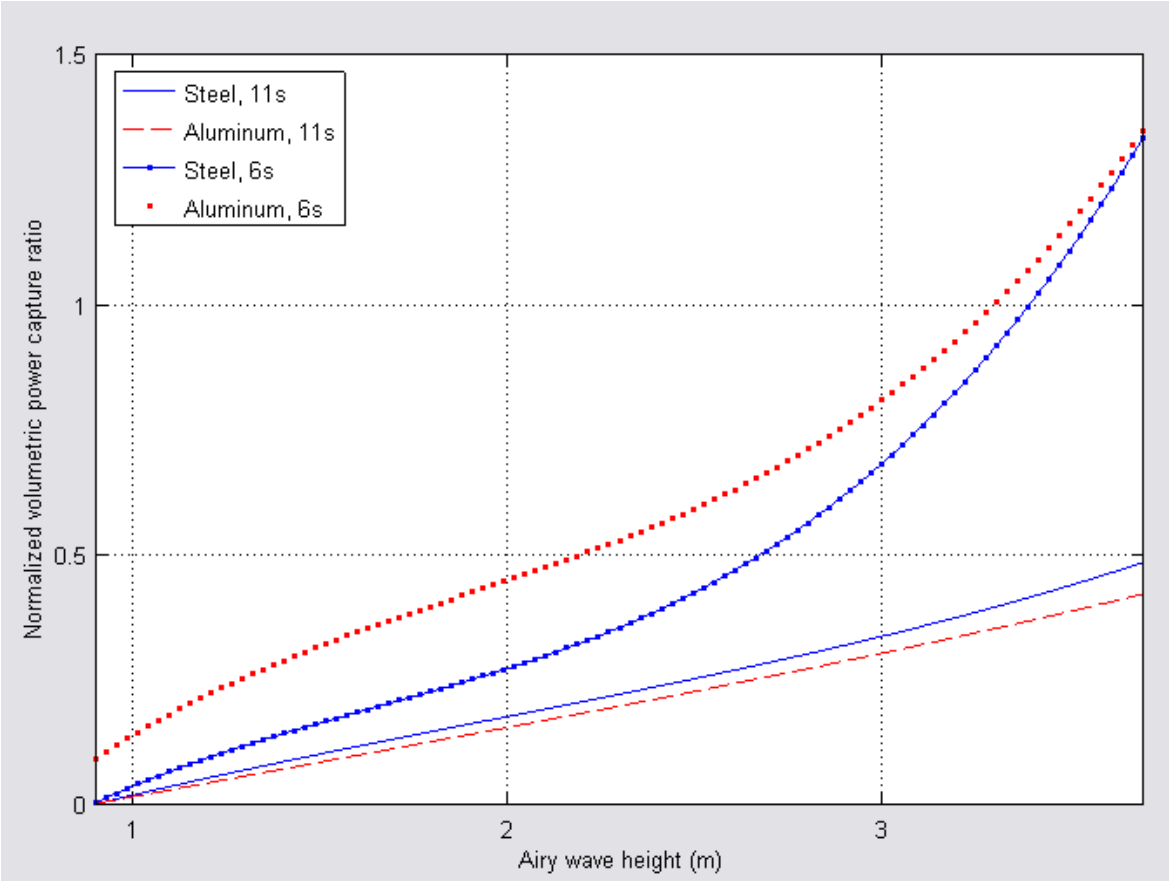

Figure 20: Dimensionless volumetric power capture ratio variation with Airy wave height

During the initiation of the power cycle, the leading edge of the pontoon is partially submerged. This phenomenon lead to full submergence of the pontoon in some Airy wave heights at 6 s period. This is likely due to the inertia of the system struggling against the smaller wave periods. To highlight this effect, the reserve buoyancy of the pontoon is shown for the largest wave heights in Figure 21. Note in this Figure that time is nondimensionalized by the wave period for each case, which allows the reserve buoyancy curves to match in phase on the plot. Since drag loading will increase as the pontoon is submerged, higher system loading and increased losses are likely. The drag losses and inertia of the system explains why the power capture of the pontoon never reaches the ideal increase factor of 1.8 in power output accounting for the higher frequency waves.

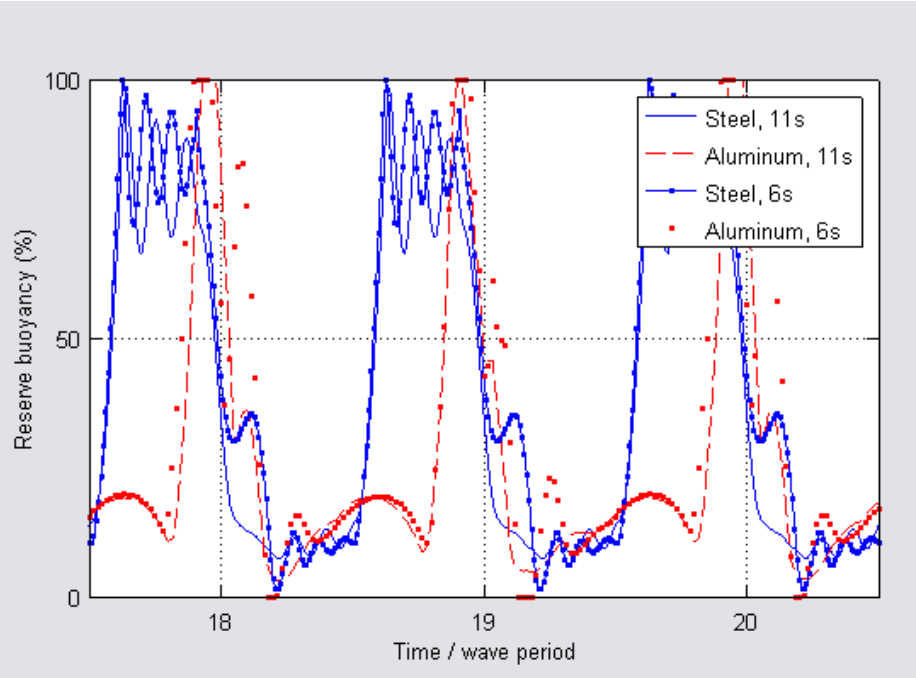

Figure 21: Pontoon reserve buoyancy in 3.7m Airy waves. Note dimensionless time scale.

Steady state cylindrical joint angle, extension, and extension velocity parameters for each pontoon and the specific sea state are summarized in Table 7. Aluminum pontoon cylinder extension velocity is faster in smaller period waves, which is due to the lower inertia when compared to the steel pontoon.

Table 7: SurfPower operational characteristics

Configuration	Downstream cylinder angle (deg)	Upstream cylinder angle (deg)	Extension amplitude (m)	Extension velocity (m/s)
Steel, 3.7 m, 11s wave	-18.0	17.0	3.6	2.1
Aluminum, 3.7m, 11s wave	-16.0	17.0	3.4	2.0
Steel, 3.7 m, 6s wave	-25.0	4.2	2.9	4.6
Aluminum, 3.7m, 6s wave	-25.0	3.4	3.1	4.9

4.3.2 Performance in multifrequency sea state

The power capture curve of the system in a multifrequency sea state can be seen in Figure 22. The

sea state consisted of 13 discrete frequencies dictated by a JONSWAP spectrum. The waves had randomly generated initial phases and their direction was randomly distributed through a swept range of 45 degrees about a mean heading. While the total power captured by the steel unit is larger than the aluminum, the power capture density again favors the aluminum pontoon over the steel pontoon, as indicated in Figure 23.

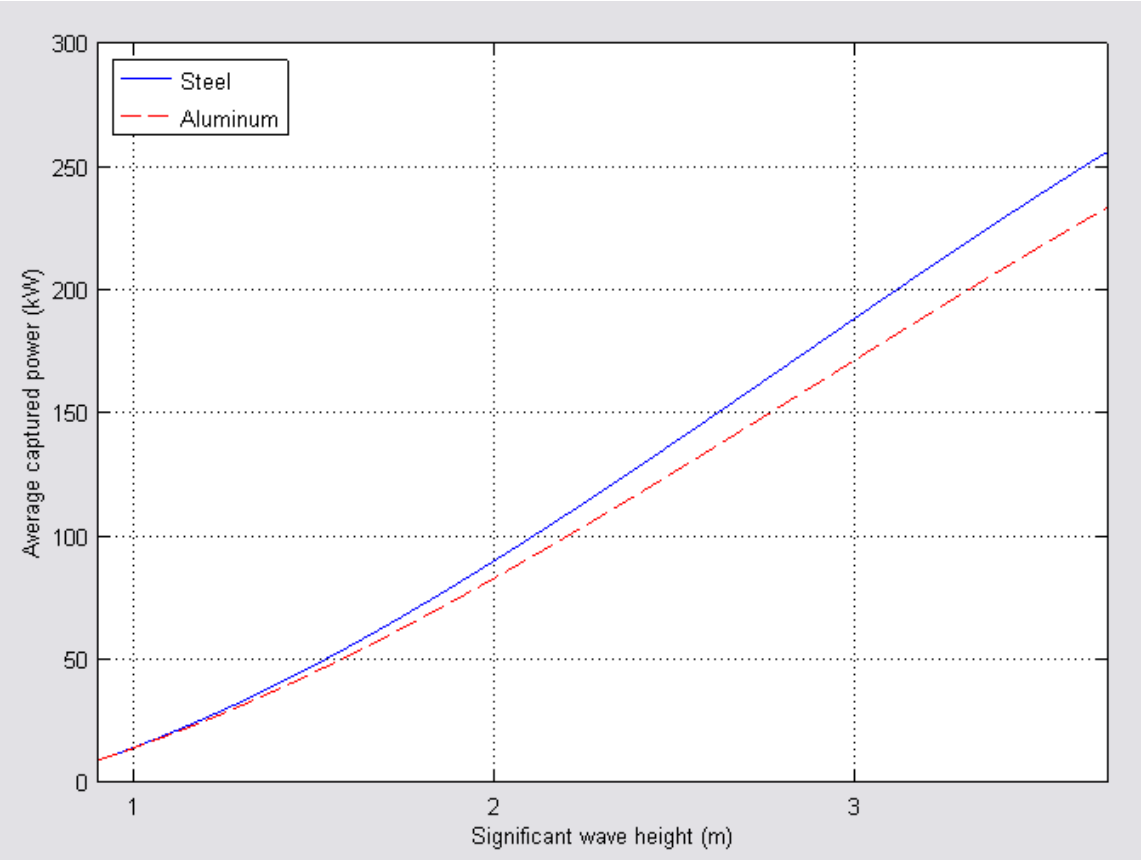

Figure 22: Power capture in multifrequency sea state with dominant period of 11 seconds

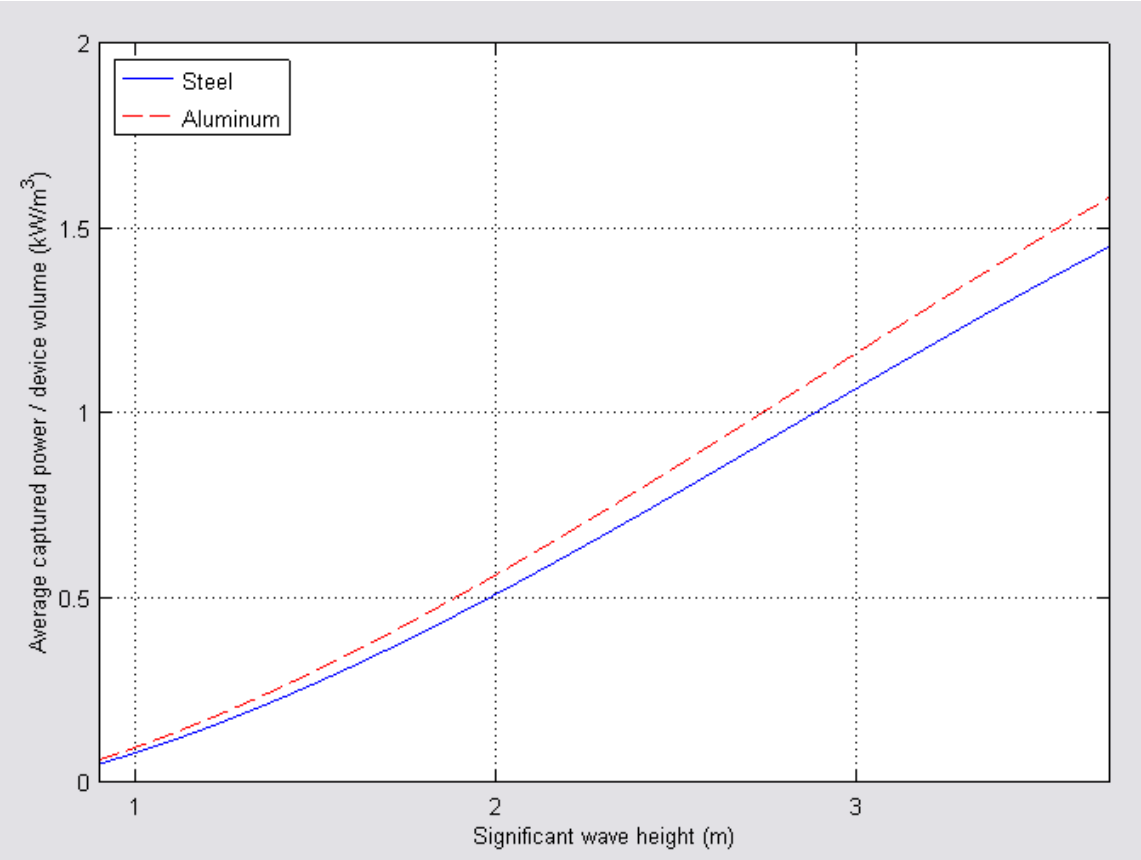

Figure 23: Power capture per unit volume of pontoon and cylinder in multifrequency sea state with dominant period of 11 seconds

The lower power production during significant wave height when compared to Airy waves is due to the variance in sea surface elevation as well as different wave direction relative to the pontoon. Significant wave height is a measure of the average of the top highest 33% of waves present in the sea state and so many waves passing the device will be lower than this value. A direct comparison highlighting this effect can be seen in Figure 24. This results in lower energy capture in the long run, though knowledge of the device performance in different multifrequency sea states is more realistic than in a monofrequency Airy wave sea state.

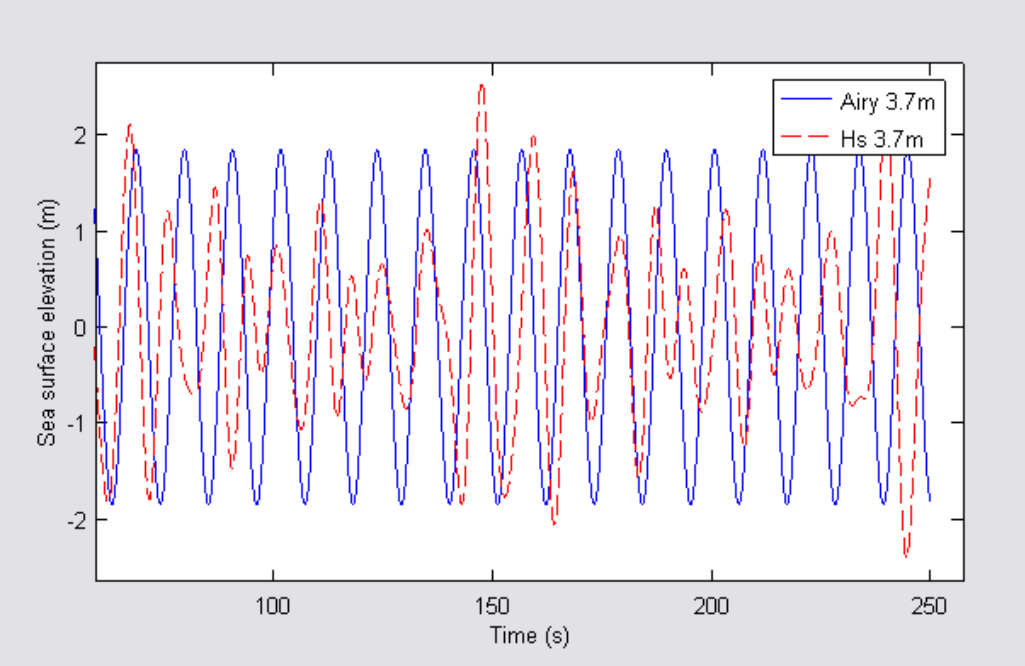

Figure 24: Mono- (Airy) and multifrequency sea state elevation comparison

4.4 Performance in extreme sea states

The system was subjected to an extreme sea state of 8 m, 15 s Airy waves. The operational characteristics of the system in these conditions are compiled in Table 8. One reason for the larger upstream cylinder angle, or overshoot on the return cycle, is due to the device's ability to 'surf' down the back of the wave. Since the draft of the device reduces significantly after the power stroke is completed, the wetted area reduces along with drag loading. The longer period and higher elevation provides more time for the pontoon to reach the trough of the oncoming wave through its own weight when compared to other waves of shorter period.

Due to the extreme conditions, a sensitivity study was completed to observe the joint extension change with hydraulic system pressure, which can be seen in Figure 25. This shows that the Aluminum pontoon responds faster to smaller increases in hydraulic pressure in reducing the joint throw when compared to the steel pontoon. This shows that both steel and aluminum pontoons will have to increase the hydraulic system pressure by approximately 15% to reduce the joint throw to the allowable 5.5 m. This does not consider the mean joint position. However, since the pontoon joint throw is very sensitive to increases of hydraulic pressure, likely only a small additional pressure increase will be required to prevent the end-stop condition from occurring. These small pressure increases may be realized by slightly reducing the turbine nozzle opening to elevate the system operating pressure.

Table 8: SurfPower operational characteristics

Configuration	Downstream cylinder angle (deg)	Upstream cylinder angle (deg)	Extension amplitude (m)	Extension velocity (m/s)
Steel, 8 m, 15s wave, 1375 psi	-20.0	25.0	7.4	2.5
Aluminum, 8m, 15s wave, 1250 psi	-18.0	21.0	7.4	2.2

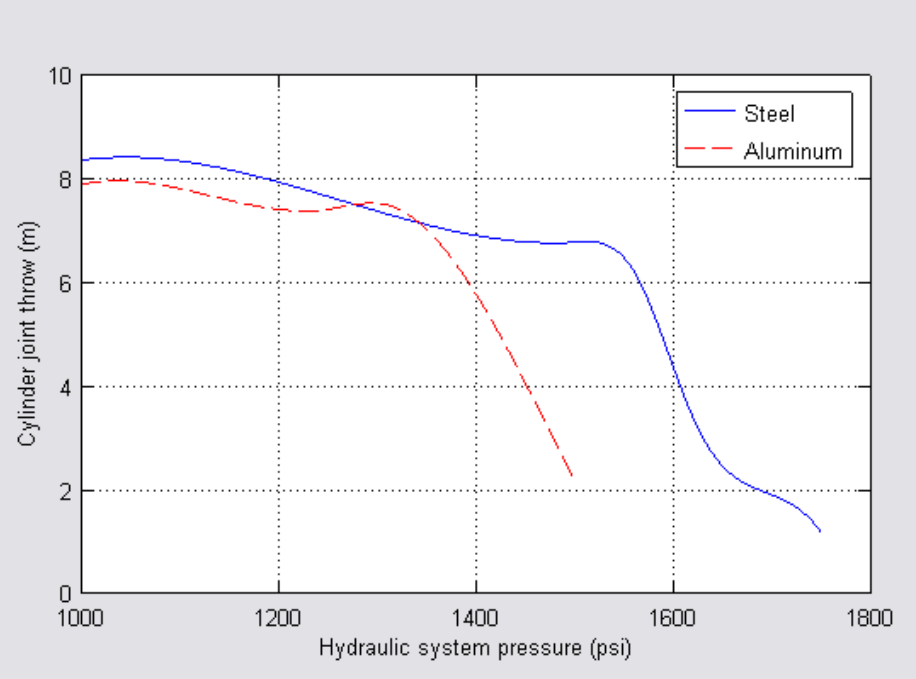

Figure 25: Cylinder joint throw decrease with hydraulic pressure increase in 8m, 15s Airy waves

A sensitivity study was performed in regard to offset values of 1.22 m, 1.98 m, and 2.74 m connection distance from the center of the pontoon to the top of the cylinder. The results showed negligible differences in the pontoon dynamic pitch angle and the pontoon does not destabilize as it passes through an oncoming 8 m wave. Power capture values were slightly higher with a smaller connection distance.

5 Conclusions

Seawood Designs (SDI) retained Dynamic Systems Analysis (DSA) to dynamically model the SurfPower system using ProteusDS software. The objective was to conduct parametric studies to refine the design and minimize the complexity and cost of tank trials in the next phase of development. Seawood Designs has found the following ProteusDS output to be very useful.

5.1 Power / Energy output

The power and energy curves closely matched energy recovery estimates previously developed by SDI. High power densities of 4 kW/m^3 (per unit volume of the pontoon and pump cylinder) in 3.7 m, 6 s and 11 s Airy waves were obtained. Similarly, 1.5 kW/m^3 was generated in a multifrequency sea state with a significant wave height of 3.7 m.

Reported energy recovery values are likely underestimated in that a conservative drag coefficient value of 1.0 and an added mass coefficient of 1.0 were used in the model.

5.2 Dynamic freeboard

Employing a minimum dynamic freeboard consistent with maximum energy recovery leads to optimizing the cost of energy delivered by SurfPower. Dynamic freeboard can usefully be defined as a percentage of the combined static pontoon draft and hydraulic freeboard. The optimum freeboard for the aluminum pontoon configuration in these studies is 6.3% and 8.1% for the steel pontoon.

5.3 Deployment depth

Sensitivity studies showed a slight decrease in energy recovery with increasing depth. It appears this is caused by a reduction in wave steepness (slope) in deeper waters, making it more difficult for the pontoon to travel during the return stroke. For waves of constant height and period, the governing physics of ocean waves dictate the wavelength decreases as the depth decreases, which is taken into account in the ProteusDS software. The resulting input is useful for SDI in that they can now entertain deployment of more than one rank of pontoon parallel to the shore and thereby increase pontoon density per kilometer of shoreline.

5.4 Optimum operating pressure

Optimum operating pressures were established for the two pontoons: 1250 psi for the aluminum pontoon and 1375 psi for the steel pontoon. These pressures act on an effective piston pump area of 200 in^2 developing system mooring loadings of 250,000 lbf and 275,000 lbf, respectively.

It was found that a small increase in operating pressure of approximately 15% greatly decreases pump stroke and the corresponding energy yield. SurfPower makes use of this characteristic to limit stroke and power in sea states above the rated 3.7m waves. Extreme conditions of 8m, 15s waves were modeled to confirm survival under these conditions.

5.5 Offset distance

Studies indicated the system was generally insensitive to changes in offset over the range of values

studied.

5.6 Sway resonance

Unexpectedly, ProteusDS identified the presence of sway resonance in some operating conditions with both aluminum and steel pontoons. Even though the system has a high level of damping that limits excursions, sway resonance did adversely impact energy yield. It does not appear that circumventing resonant conditions by knowledgeable designers will be a problem. Foreknowledge in this circumstance is invaluable.

5.7 Influence of pontoon mass

Two pontoons with significantly different mass were used in the studies: the steel pontoon was almost twice the mass of the aluminum pontoon. As expected, the aluminum pontoon performed better especially in lower period waves (6 s).

5.8 Pump cylinder angular deflection from vertical

The maximum value projected by ProteusDS was 25 degrees. SurfPower component designs previously anticipated maximum deflections of 30 degrees.

5.9 Peak piston velocity / system flow velocity

ProteusDS anticipated the maximum piston velocity in 3.7 m, 11 s waves at 2.1 m/s that delivers a flow velocity of about 6.3 m/s. A peak piston velocity of 4.9 m/s is experienced with the aluminum pontoon in 6 s seas with a corresponding flow velocity of 14.7 m/s. SDI has commented that 6 s flow rates are excessive and will have to be reduced by increasing the internal diameter of the piston rod. However, some excessive head loss under these conditions due to high flow will help keep the system output close to the rated capacity when operating in wave conditions with shorter periods.

5.10 Operation in confused seas

A run was executed with the tapered pontoon operating in a sea state with waves approaching from directions orthogonal to each other. The pontoon was found capable of following the surface and generating power in excess of that normally delivered by the more powerful waves in a single direction alone.

6 References

O.M. Faltinsen, Sea Loads on Ships and Offshore Structures, Cambridge University Press, 1990

Radhakrishnan, S; Datla, R; Hires, R. I. Theoretical and experimental analysis of tethered buoy instability in gravity waves. Ocean engineering, 2007, 34, 261-274.

Hem Lata, W.; Thiagarajan, K. P. Comparison of added mass coefficients for a floating tanker evaluated by conformal mapping and boundary element methods. 16th Australasian Fluid Mechanics Conference (AFMC), 2007, 1388-1391.